SAND2022-15692C

Impact of Extreme Weather on Sizing Battery Energy Storage Systems: A Case Study of Fairbanks, Alaska

Walker Olis
Electric Power Systems Research Department
Sandia National Laboratories
Albuquerque, NM, USA
wolis@sandia.gov

***Abstract*—Efficient operation of battery energy storage systems (BESSs) requires a limited battery temperature range. The effects of parasitic heating and cooling loads on the optimal sizing of BESSs are investigated in this paper. Peak shaving is presented as a linear programming (LP) problem formulated in the PYOMO optimization programming language. The building energy simulation software EnergyPlus models the heating, ventilation, and air conditioning (HVAC) load of the BESS enclosure. A case study is analyzed in Fairbanks, Alaska, considering a lithium nickel manganese cobalt oxide (NMC) battery type and whether the power conversion system (PCS) is inside or outside the enclosure. The analysis illustrates that the HVAC load can have a large impact on the optimal energy and power capacities of an energy storage system and that insulating and including the PCS in the enclosure can reduce overall costs.**

***Index Terms*—battery energy storage system, energy storage, energy storage sizing, thermal management, extreme climates**

I. Introduction

BATTERY ENERGY STORAGE SYSTEMS are a key technology reducing fossil fuel consumption and providing reliable energy. Renewable generation becomes more attractive when paired with BESSs due to their intermittency [1]. Careful attention must be given to the operating temperature of these devices as they are easily damaged when outside the optimal range. While this is well known, analytical studies often neglect these problems by assuming the batteries operate at a constant temperature. This work attempts to alleviate this issue by including an estimate of the heating, ventilation, and air conditioning (HVAC) load of the BESS enclosure. This study focuses on optimal sizing and operation of BESS for a peak shaving application in Fairbanks, Alaska. Including the parasitic HVAC load of the enclosure provides an improved estimate of the energy requirements of the system.

This research was funded by the Department of Energy, Office of Electricity Energy Storage Program. This paper describes objective technical results and analysis. Any subjective views or opinions that might be expressed in the paper do not necessarily represent the views of the U.S. Department of Energy or the United States Government.

Sandia National Laboratories is a multimission laboratory managed and operated by National Technology & Engineering Solutions of Sandia, LLC, a wholly owned subsidiary of Honeywell International Inc., for the U.S. Department of Energy's National Nuclear Security Administration under contract DE-NA0003525.

Sizing ESSs has been extensively researched in multiple areas such as renewable energy firming, demand response, and microgrids. Optimal sizing of BESSs with a PV plant is presented in [2] to maximize revenue of the PV-BESS pair. In [3], PV-BESS size, operation, and energy management is optimized to generate revenue with consideration of the capacity of grid connection. A Discrete Fourier Transform (DFT) approach is proposed in [5] to size a hybrid ESS containing battery energy storage and pumped hydropower to mitigate wind power fluctuations. In [6] a comprehensive study was performed on the optimal size, technology, and depth of discharge of battery energy storage to reduce the microgrid operational cost and improve reliability. This work builds on the results in [7] to improve the expected lifetime of a BESS and analyze the effects of microgrid participation in energy markets.

The previous studies neglect the parasitic heating and cooling loads of the BESS enclosure. In particular, BESS must be kept within an operating temperature range to ensure optimal performance and in many cases maintain the warranty. While neglected in grid scale models, battery control models include temperature when it can affect battery operation. An equivalent circuit model considering thermal effects for Vanadium Redox Flow (VRB) BESSs is developed in [8] using a third order Cauer network for the thermal circuit. The model is experimentally validated with a 5kW/3kWh system and then used in a simulation supporting a wind power plant. In [9], a comprehensive review of optimal battery control strategies is presented. Section IV in [9] describes temperature modeling and shows that optimal control of the battery and HVAC unit setpoints provide an electricity bill reduction while keeping the battery temperature within operating range. A comparative study of control-oriented thermal models for lithium-ion batteries in vehicle and grid applications is presented in [10]. The models are evaluated in situations where both core and surface temperature are known and also where only the surface temperature is known using simulations and experimental data sets of lithium iron phosphate (LFP) batteries. The polynomial approximation (PA) is found to be the best model in practical applications when considering model assumptions, model

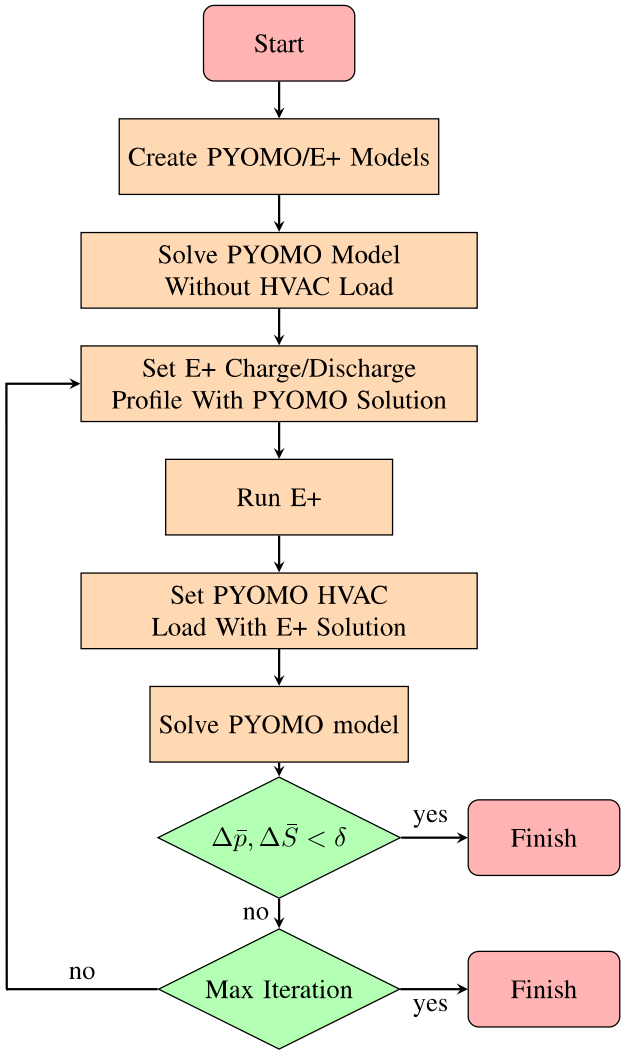

Fig. 1. Iterative solution flow chart.

fidelity, computational cost, and model sensitivity.

In this paper, a new method is proposed to calculate the optimal size of a BESS considering the local climate. This method is coded in python and uses the PYOMO optimization programming language [11], [12] and the building energy simulation software EnergyPlus [13], [14]. Analysis of a case study in Fairbanks, Alaska, shows an improved sizing estimate in extreme climates along with quantitative estimates of the cost savings achievable with different levels of insulation and by including the PCS inside the BESS enclosure.

II. Methodology

This algorithm is designed such that the optimization model is interchangeable so long it takes HVAC power as an input and ouputs a BESS charge/discharge profile. Similarly, any EnergyPlus input file is usable so long as there is a suitable location for the BESS. PCS placed inside or outside the enclosure will determine whether to include PCS inefficiency in the heat balance. PYOMO [11], [12] and EnergyPlus models are created for the optimization and heat balance

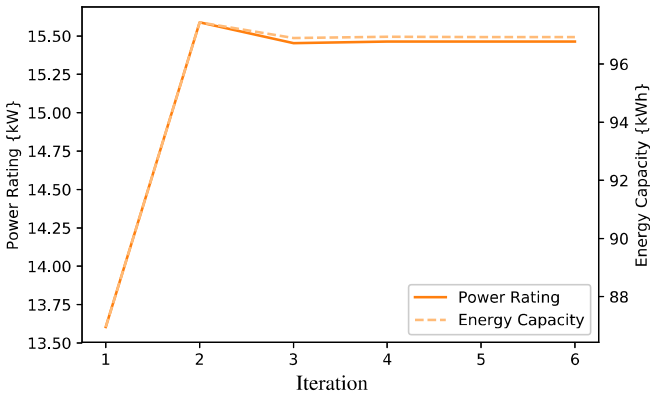

Fig. 2. Power Rating and Energy Capacity of a BESS in Fairbanks, Alaska, with R-13 insulation. The values converge at the sixth iteration.

models, respectively. The PYOMO model is then solved with no consideration for the HVAC load to provide the BASE solution. The charge-discharge profile from the BASE solution is given to an EnergyPlus simulation, which solves for the HVAC load to update the PYOMO model. Convergence is not guaranteed as the relationship between BESS parameters and HVAC load solution is nonlinear and non-convex. Therefore, the process is repeated until the energy capacity and power rating of the BESS and the power rating of the PV meet convergence criteria or a maximum number of iterations are run. In Fig. 2 parameters are shown to rapidly converge. This provides the minimum sized BESS at a certain location. A flow chart describing this process is shown in Fig. 1. In this case, a BESS inside a shipping container is considered providing peak shaving to a customer in Fairbanks, AK.

A. LP Formulation

The size optimization model seeks to minimize the capital costs of the BESS and the cost of energy:

$$\min \quad C^Q_{BESS} Q_{BESS} + C^P_{BESS} P_{BESS} + C_E \tag{1}$$

where Q_{BESS} is the rated energy capacity of the BESS and P_{BESS} is the power rating of the BESS. C^Q_{BESS}, C^P_{BESS}, and C_E are the cost per battery MWh, battery MW, and cost of electricity. The model is subject to constraints:

$$q_i^d + q_i^{\text{grid}} - q_i^c = q_i^{\text{load}} + q_i^{\text{hvac}}, \forall i \in \mathbf{A} \tag{2a}$$

$$q_i^c + q_i^{\text{grid}} \leq q^{\max}, \forall i \in \mathbf{A} \tag{2b}$$

where q_i^d, q_i^{grid}, q_i^c, q_i^{load}, and q_i^{hvac} are the discharge, grid, charge, load, and HVAC energy respectively at each time step.

B. Energy Reservoir Model

The ERM assumes a linear relationship between stored and transferred energy, formulated as follows:

$$S_i = n^s S_{i-1} + n^{\text{rt}} q_i^c - q_i^d, \forall i \in \mathbf{A} \tag{3}$$

where S_i is the state of energy (MWh) at the i^{th} timestep of length τ (hr). The storage efficiency n^s and round trip efficiency n^{rt} are assumed constant while the charge energy q^c

(MW) and discharge energy q^d (MW) are the average value over the time step and defined to be nonnegative. The ESS device is also constrained by

$$0 \leq q_i^c + q_i^d \leq Q, \forall i \in \mathbf{A} \tag{4a}$$

$$S_{\min} \leq S_i \leq S_{\max}, \forall i \in \mathbf{A} \tag{4b}$$

$$\sum_{i \in A} n^{rt} q_i^c - q_i^d = 0. \tag{4c}$$

The constraint (4a) ensures charge and discharge profile is within BESS limits. The constraint (4b) requires the state of charge of the system to be within a specified range. The constraint (4c) requires the net charging to be zero. The complimentary slackness constraint is not included because it is assumed any simultaneous charging and discharging would be settled within the time period.

C. EnergyPlus

EnergyPlus is a building simulation software used to model energy consumption developed by the US Department of Energy's Building Technology Office and first released in April of 2001. The software has been widely adopted as a leader in building energy simulation. The Energy Plus input file, or IDF, contains all of the details pertaining to the building's energy and mass transfer. Typically, standalone battery energy storage devices are housed in shipping containers. Standard high cube units are constructed with lengths of 10', 20', and 40', with a standard width and height of 8' x 9'6". The walls and doors consist of a 2mm layer corten steel while the floor is a 28 mm layer of marine plywood fastened on top of steel crossbars [16]. HVAC units are compound objects built with individually modeled components in EnergyPlus. For this study, a packaged terminal air conditioner (PTAC) is modeled within the shipping container enclosure. The PTAC is a single unit with both heating and cooling capabilities. The configuration consists of an outdoor air mixer, electric heating coil, direct expansion cooling coil, and fan.

D. Non-linear ERM

A non-linear energy flow model specific to lithium-ion and lead-acid batteries is used to describe the heat loss of the battery. The non-linear formulation of (3) is expressed as [17]:

$$S_i = n^s S_{i-1} + \tau f_i^c(p_i^c, S_{i-1}) - \tau f_i^d(p_i^d, S_{i-1}) \tag{5}$$

where f^c and f^d represent the average charged and discharged power over a time step. The system level rate of energy loss can be formulated as [17]:

$$\begin{aligned} p_i^{ld} &\approx \frac{\bar{q}}{\bar{v}\bar{S}}[(r + \frac{k\bar{S}}{S_i})(\frac{p_i^d}{n^p})^2 + \frac{k\bar{S}(\bar{S} - S_i)}{S_i}\frac{p_i^d}{n^p}] \\ &= p_i^R + p_i^V \end{aligned} \tag{6}$$

$$\begin{aligned} p_i^{lc} &\approx \frac{\bar{q}}{\bar{v}\bar{S}}[(r + \frac{k\bar{S}}{\bar{S} - S_i})(n^p p_i^c)^2 + \frac{k\bar{S}(\bar{S} - S_i)}{S_i} n^p p_i^c] \\ &= p_i^R + p_i^V \end{aligned} \tag{7}$$

where $\bar{S}$ is the rated energy capacity of the system, $\bar{q}$ as the rated ampere-hour capacity of a battery cell, $\bar{v}$ as the rated voltage of a battery cell, r as the internal resistance of a battery cell, n^p as the power conversion system efficiency, and the model coefficient k can be calculated from nameplate or testing data [17]. Then the charged and discharged power at each time step is the sum of consumed power and power loss:

$$f_i^d = \frac{p_i^d}{n^p} + p_i^{ld} \tag{8}$$

$$f_i^c = n^p p_i^c - p_i^{lc} \tag{9}$$

The energy lost as heat to the enclosure is given by the p_i^R terms in equations (6) and (7) representing the power losses due to ohmic and polarization resistances. This heat is released into the enclosure model using the EnergyPlus API.

III. Case Study

A NMC battery is considered with characteristics shown in table I. Scenarios where the PCS is considered to be inside the enclosure is also simulated, with the inefficiency is considered to be lost as heat. The enclosure temperature is kept between the operating range of the battery shown in Table I. It is assumed that the battery temperature is equal to the ambient temperature of the enclosure.

TABLE I
LG 18650 Characteristics [18], [19]

Chemistry	NMC
$\bar{q}$	2.5 Ah
$\bar{v}$	3.6 V
r	0.02 Ω
k	0.005 Ω
Temperature Range	15-40 °C

An hourly load profile representing a warehouse is used and considered to be constant throughout each hour, accessible from [20]. The TMY3 weather file is used and accessible from the EnergyPlus website [13]. The capital costs described in (1) are determined using a regression algorithm on the data presented in [21] as 132.36 $\frac{\$}{kW}$ and 360.38 $\frac{\$}{kWh}$. The storage, round-trip, and PCS efficiency are 100%, 83.32%, and 93.32% respectively. The rate structure of AKF has a constant energy charge of 0.12638 $\frac{\$}{kWh}$ and constant demand charge of 22.27 $\frac{\$}{kW}$ throughout the year [22]. The total load is shaved to 70 kW by the BESS. The amount of insulation in the shipping container is varied from 0-3 $\frac{m^2K}{W}$. The simulations are annual with a time step of fifteen minutes.

The BASE scenario in which the parasitic HVAC loads are not included in the sizing optimization results in a BESS with an energy capacity of 86.9 kWh and power rating 13.6 kW. Fig. 3 shows the resulting sizes considering the PCS to be inside or outside the enclosure for a range of insulation values. Without any insulation the BESS triples to 261.6 kWh, 29.6 kW when PCS is considered outside of the enclosure. When PCS is inside the enclosure the size reduces to 220.1 kWh, 28.4 kW. As insulation is added to the shipping container, the sizes decay exponentially toward the BASE value. The common wall value insulation R-13 (approximately 2.3 $\frac{m^2K}{W}$)

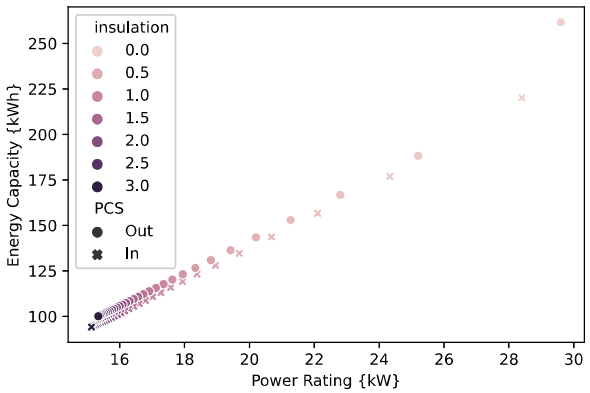

Fig. 3. BESS size in Energy Capacity and Power Rating as the insulation is varied from 0 to 3 $\frac{m^2K}{W}$.

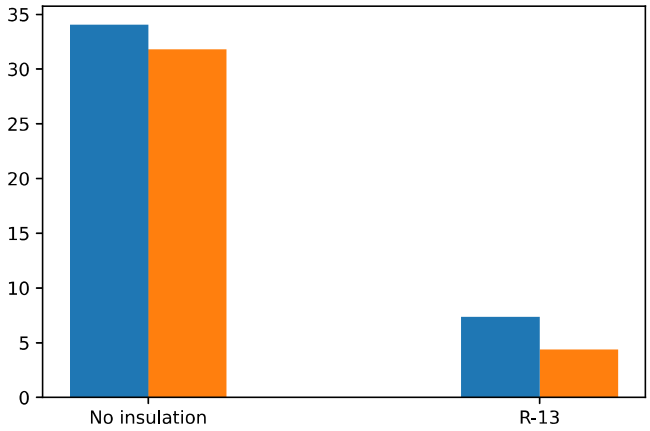

Fig. 5. Percent of BESS energy consumption used toward the HVAC load.

reduces the BESS size to 103 kWh, 15.7 kW with PCS outside the container and 96.9 kWh, 15.5 kW with PCS inside the container.

Similarly, as shown in Fig. 4 the capital cost of the BESS exponentially decays from the case without insulation at $98,211 with PCS outside the enclosure toward the BASE cost at $33,137. The optimal battery capital cost with standard R-13 insulation is $39,197 with PCS outside the enclosure and $36,980 with PCS inside the enclosure. A comparison of the energy bill with different levels of insulation is also shown in Fig. 4. The BASE case predicts $659 of annual savings. Considering parasitic loads with no insulation and PCS outside of the enclosure the energy bill is more expensive by $5,479. The break even point is at 2.7 RSI when the BESS will save $10 over the course of the year.

Fig. 5 shows the percentage of BESS energy used to power the HVAC in the case when there is no insulation in the shipping container and with R-13 insulation. Without insulation, the HVAC consumes 34% of the discharged BESS energy when PCS is considered outside of the enclosure and 31.8% when PCS is inside the enclosure. With standard R-13 insulation there is a significant reduction to 7.4% and 4.4% when PCS is outside and inside respectively.

The temperature in Fairbanks, Alaska, is regularly below -20 °C in the winter, even approaching -40 °C. This is apparent in Fig. 6 which displays the daily consumption of energy by the BESS and HVAC over the course of the year when the shipping container is not insulated along with the case where it is insulated with R-13. In both cases, consumption of energy peaks during the winter months. Without insulation this effect is drastic leading to the larger system size. Using R-13 in the enclosure substantially reduces HVAC consumption from a peak of over 350 kWh to around 50 kWh. This translates to BESS consumption, where the R-13 insulation reduces the energy used during the winter months approximately by half.

Parasitic heating and cooling loads increase the amount of energy needed to operate BESSs necessitating a larger size for the desired application. While peak shaving is a simple example, the point is illustrated well by the results. Insulating the enclosure provides an enormous benefit. Using

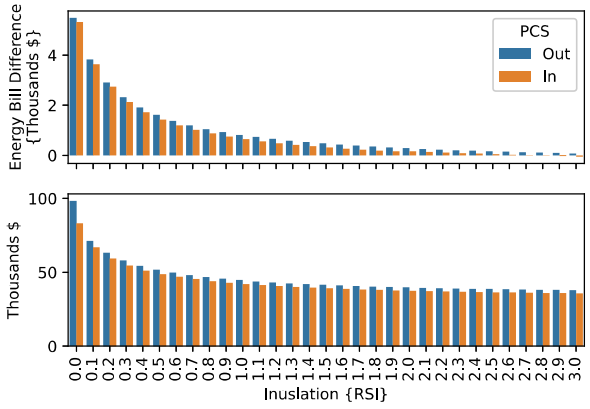

Fig. 4. Change in energy bill compared with the warehouse base load (top) and BESS capital cost (bottom) as the insulation is varied from 0 to 3 $\frac{m^2K}{W}$.

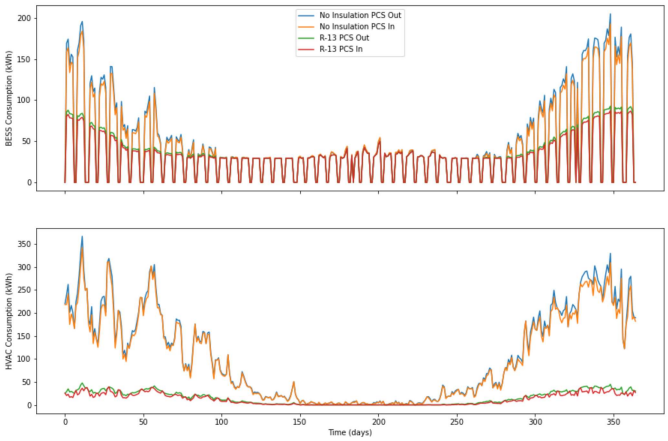

Fig. 6. Daily BESS (top) and HVAC (bottom) usage of energy.

the standard wall insulation R-13, the system size is reduced by approximately 60% in energy capacity and 45% in power rating regardless of whether the PCS is outside or inside the enclosure saving approximately $60,000 and $50,000 respectively. Savings in capital costs is also achievable by placing PCS inside the enclosure at an average of 6% regardless of insulation. Results show a more expensive annual energy bill in this scenario, indicating peak shaving may not be economically viable.

Topics for future consideration include locational dependence, degradation, and rate structure. The location is likely to have the most profound effect as the extremity of the climate is expected to control the BESS size. Degradation would be interesting as the increase in HVAC consumption increases the usage of the BESS likely leading to a shorter lifespan. Including a battery temperature model would likely constrain operation further. Using local rate structures adds further complexity and may only significantly alter the results when the BESS heat loss and HVAC consumption are comparable, in which case the BESS operation will affect when the largest parasitic loads occur. Different use cases of the BESS would likely affect the overall economics and would be interesting future work, however it is beyond the scope of this paper.

IV. Conclusion

The effects of parasitic heating and cooling loads on BESS sizing are investigated in this paper. Sizing problems are formulated for the peak shaving case. HVAC loads are incorporated using EnergyPlus to model a BESS enclosure, namely a shipping container with a PTAC unit in Fairbanks, Alaska, considering an NMC lithium-ion battery type and whether the PCS is inside or outside the enclosure. Results show that a larger battery capacity is required than would be anticipated without considering parasitic HVAC loads to provide the same functionality. Placing PCS inside the BESS enclosure and insulating the shipping container can result in significant savings on capital costs and a reduction in HVAC consumption over the entire year. This analysis illustrates the importance of accounting for local climate and consequent parasitic loads when considering the usage of BESS.

V. Acknowledgments

The author would like to thank Dr. David Rosewater, Dr. Tu Nguyen, and Dr. Raymond Byrne for their guidance and useful discussions.

This article has been authored by an employee of National Technology & Engineering Solutions of Sandia, LLC under Contract No. DE-NA0003525 with the U.S. Department of Energy (DOE). The employee owns all right, title and interest in and to the article and is solely responsible for its contents. The United States Government retains and the publisher, by accepting the article for publication, acknowledges that the United States Government retains a non-exclusive, paid-up, irrevocable, world-wide license to publish or reproduce the published form of this article or allow others to do so, for United States Government purposes. The DOE will provide public access to these results of federally sponsored research in accordance with the DOE Public Access Plan https://www.energy.gov/downloads/doe-public-access-plan.

References

[1] Y. Tian, A. Bera, M. Benidris, and J. Mitra, "Reliability and environmental benefits of energy storage systems in firming up wind generation," in *2017 North American Power Symposium (NAPS)*, 2017, pp. 1–6.

[2] S. Oh, J. Kong, W. Lee, and J. Jung, "Development of optimal energy storage system sizing algorithm for photovoltaic supplier in south korea," in *2018 IEEE Power Energy Society General Meeting (PESGM)*, 2018, pp. 1–5.

[3] Y. Yoo, G. Jang, and S. Jung, "A study on sizing of substation for pv with optimized operation of bess," *IEEE Access*, vol. 8, pp. 214 577–214 585, 2020.

[4] M. R. Narimani, B. Asghari, and R. Sharma, "Optimal sizing and operation of energy storage for demand charge management and pv utilization," in *2018 IEEE/PES Transmission and Distribution Conference and Exposition (T D)*, 2018, pp. 1–5.

[5] I. N. Moghaddam and B. Chowdhury, "Optimal sizing of hybrid energy storage systems to mitigate wind power fluctuations," in *2016 IEEE Power and Energy Society General Meeting (PESGM)*, 2016, pp. 1–5.

[6] I. Alsaidan, A. Khodaei, and W. Gao, "A comprehensive battery energy storage optimal sizing model for microgrid applications," *IEEE Transactions on Power Systems*, vol. 33, no. 4, pp. 3968–3980, 2018.

[7] A. M. Alharbi, W. Gao, and I. Alsaidan, "Sizing battery energy storage systems for microgrid participating in ancillary services," in *2019 North American Power Symposium (NAPS)*, 2019, pp. 1–5.

[8] B. Xiong, Y. Yang, J. Tang, Y. Li, Z. Wei, Y. Su, and Q. Zhang, "An enhanced equivalent circuit model of vanadium redox flow battery energy storage systems considering thermal effects," *IEEE Access*, vol. 7, pp. 162 297–162 308, 2019.

[9] D. M. Rosewater, D. A. Copp, T. A. Nguyen, R. H. Byrne, and S. Santoso, "Battery energy storage models for optimal control," *IEEE Access*, vol. 7, pp. 178 357–178 391, 2019.

[10] X. Hu, W. Liu, X. Lin, and Y. Xie, "A comparative study of control-oriented thermal models for cylindrical li-ion batteries," *IEEE Transactions on Transportation Electrification*, vol. 5, no. 4, pp. 1237–1253, 2019.

[11] W. E. Hart, J.-P. Watson, and D. L. Woodruff, "Pyomo: modeling and solving mathematical programs in python," *Mathematical Programming Computation*, vol. 3, no. 3, pp. 219–260, 2011.

[12] W. E. Hart, C. D. Laird, J.-P. Watson, D. L. Woodruff, G. A. Hackebeil, B. L. Nicholson, and J. D. Siirola, *Pyomo–optimization modeling in python*, 2nd ed. Springer Science & Business Media, 2017, vol. 67.

[13] U. S. Department of Energy, "Energy plus building simulation software," 2020. [Online]. Available: https://energyplus.net/

[14] D. Crawley, C. Pedersen, L. Lawrie, and F. Winkelmann, "Energyplus: Energy simulation program," *Ashrae Journal*, vol. 42, pp. 49–56, apr 2000.

[15] D. Crawley, L. Lawrie, F. Winkelmann, and C. Pedersen, "Energyplus: A new-generation building energy simulation program," in *Proceedings of FORUM 2001: Solar energy: the power to choose*. American Solar Energy Society, apr 2001.

[16] G. Elrayies, "Thermal performance assessment of shipping container architecture in hot and humid climates," *International Journal on Advanced Science, Engineering and Information Technology*, vol. 7, p. 1114, 08 2017.

[17] T. A. Nguyen, D. A. Copp, R. H. Byrne, and B. R. Chalamala, "Market evaluation of energy storage systems incorporating technology-specific nonlinear models," *IEEE Transactions on Power Systems*, vol. 34, no. 5, pp. 3706–3715, 2019.

[18] "Technical information of lg 18650he2." [Online]. Available: {https://www.powerstream.com/p/LG%2018650HE2%20Technical%20Information.pdf}

[19] *IEEE/ASHRAE 1635-2018*, May 2018.

[20] "Commercial and residential hourly load profiles for all tmy3 locations in the united states." [Online]. Available: https://openei.org/datasets/files/961/pub/COMMERCIAL_LOAD_DATA_E_PLUS_OUTPUT/USA_AK_Fairbanks.Intl.AP.702610_TMY3/

[21] R. Baxter, "2019 energy storage pricing survey," Sandia National Laboratories, Albuquerque, NM, Tech. Rep. SAND2021-0831, Jan 2021.

[22] Golden Valley Electric Association, "GVEA rate schedules," 2021. [Online]. Available: https://www.gvea.com/rates/?doing_wp_cron=1612339564.1071701049804687500000